Cluster chemistry

LIX. Stereochemistry of group 15 ligand-substituted derivatives of $M_3(CO)_{12}$ (M = Ru, Os). D *. Synthesis and characterisation of some tetra-substituted ruthenium complexes: X-ray structures of $Ru_3(CO)_8(L)_4$ (L = PMe_2Ph and $P(OR)_3$, R = Me, Et and Ph)

Michael I. Bruce *, Michael J. Liddell, Omar bin Shawkataly,

Jordan Laboratories, Department of Physical and Inorganic Chemistry, University of Adelaide, Adelaide, South Australia, 5001 (Australia)

Ian Bytheway, Brian W. Skelton and Allan H. White

Department of Physical and Inorganic Chemistry, University of Western Australia, Nedlands, Western Australia 6009 (Australia)

(Received November 23rd, 1988)

Abstract

Several tetra-substituted derivatives of $Ru_3(CO)_{12}$ have been synthesised, and the molecular structures of $Ru_3(CO)_8(L)_4$ (L = PMe_2Ph and $P(OR)_3$, R = Me, Et, Ph) have been determined by single-crystal X-ray diffraction methods. The non-carbonyl ligands occupy equatorial positions in the Ru_3 triangle, one on each of two metal atoms, and two on the third. Twisting of the ML_4 moieties about the Ru–Ru bonds is found, leading to the presence of one μ-CO ligand in the PMe_2Ph and $P(OEt)_3$ complexes; the latter also has two semi-bridging CO ligands about the other two Ru–Ru bonds. The PMe_2Ph and $P(OEt)_3$ complexes exhibit 50/50 disorder of the Ru_3 core about a crystallographic inversion centre; the $P(OMe)_3$ complex has a similar 15/85 disorder in the Ru_3 core, and also in two of the OMe groups on one $P(OMe)_3$ ligand. A discussion of the major structural features of $M_3(CO)_{12-n}(L)_n$ (n = 1–4) is given.

Crystal data: $Ru_3(CO)_8(PMe_2Ph)_4$, triclinic, $P\bar{1}$, a 12.040(2), b 10.482(6), c 9.549(4) Å, α 86.26(4), β 69.69(3), γ 78.72(3)°, U 1108.4(6) Å^3, $Z = 1$, N_0 (number of observed data with $I > 3\sigma(I)) = 2056$, $R = 0.076$, $R' = 0.075$; $Ru_3(CO)_8\{P(OMe)_3\}_4$, monoclinic, $P2_1$, a 9.821(2), b 17.384(6), c 10.912(3) Å, β 94.88(2)°, U 1856(1) Å^3, $Z = 2$, $N_0 = 2726$, $R = 0.041$, $R' = 0.046$; $Ru_3(CO)_8\{P(OEt)_3\}_4$, monoclinic, $C2/c$, a 18.987(6), b 12.465(4), c 22.244(7) Å, β 102.03(3)°, U 5149(3) Å^3,
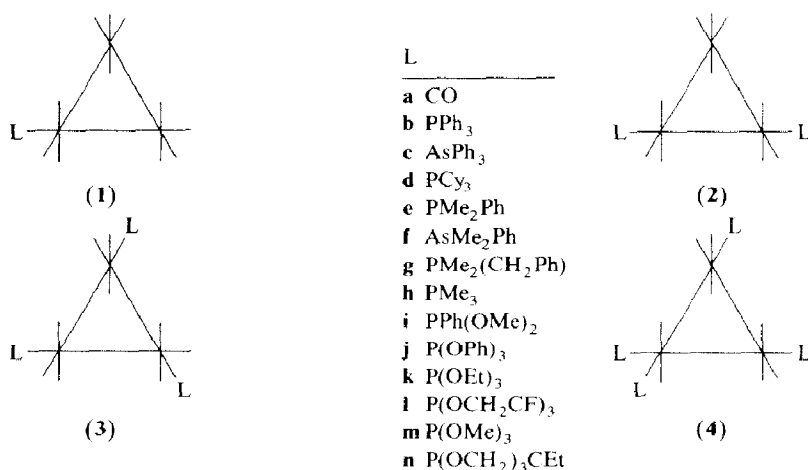
---

* For Parts A–C, see ref. 1–3.

$Z = 4$, N_0 $(I > 2\sigma(I)) = 1729$, $R = 0.066$, $R' = 0.048$: $Ru_3(CO)_8\{P(OPh)_3\}_4$, monoclinic, $P2_1/c$, a 21.14(1), b 13.820(9), c 27.24(3) Å, β 106.34(6)°, U 7637(7) Å³, $Z = 4$, N_0 $(I > 2\sigma(I)) = 6107$, $R = 0.073$, $R' = 0.052$.

Introduction

In this, the last of four papers [1-3] describing the stereochemistry of complexes $M_3(CO)_{12-n}(L)_n$ (M = Ru or Os, $n = 1-4$), we describe the synthesis and characterisation of several tetra-substituted complexes containing monodentate Group 15 ligands. Before this work, there were known only five complexes containing four or more such ligands, namely $Ru_3(CO)_8(PH_3)_4$, obtained from a reaction between $\{RuCl_2(CO)_3\}_2$ and PH_3 [4], $Ru_3(CO)_{12-n}(PF_3)_n$ ($n = 4-6$), present in the mixture of compounds obtained from $Ru_3(CO)_{12}$ and PF_3 [5], $Ru_3(CO)_8(PMe_3)_4$ [6], and $Ru_3(\mu-CO)_2(CO)_6\{PPh(OMe)_2\}_4$, described by us earlier [6,7] as the first example of a derivative of $Ru_3(CO)_{12}$ with the $Fe_3(CO)_{12}$-type structure [8]. In contrast, there are many complexes containing two bidentate tertiary phosphine or arsine ligands of formula $Ru_3(CO)_8(LL)_2$ (e.g. LL = dppm [9,10] *, dmpm [11,12], dppe [13], dppee [14], ffos [15], dpae [9], ffars [15]) and three reports of compounds $Ru_3(CO)_6(LL)_3$ (LL = dppm [16], dppe [16,17], dppee [14], pdma [17]). More recently Pomeroy and coworkers have described the extensive thermal and photolytic reactions which are required to give $Os_3(CO)_{12-n}\{P(OMe)_3\}_n$ ($n = 4-6$) [18,19].

In the account of the synthesis and characterisation of several complexes $Ru_3(CO)_8(L)_4$ that follows, we use the convention introduced in Part A [1] to label these complexes (see Scheme 1). In addition to the crystal structures of the title compounds, we also summarise the main conclusions of this study.

L	
a	CO
b	PPh_3
c	$AsPh_3$
d	PCy_3
e	PMe_2Ph
f	$AsMe_2Ph$
g	$PMe_2(CH_2Ph)$
h	PMe_3
i	$PPh(OMe)_2$
j	$P(OPh)_3$
k	$P(OEt)_3$
l	$P(OCH_2CF_3)_3$
m	$P(OMe)_3$
n	$P(OCH_2)_3CEt$

Scheme 1

* Abbreviations: dppm = $CH_2(PPh_2)_2$, dmpm = $CH_2(PMe_2)_2$, dppe = $PPh_2(CH_2)_2PPh_2$, dppee = $(PPh_2)_2C=CH_2$, ffos = $(PPh_2)C=C(PPh_2)CF_2CF_2$, dpae = $AsPh_2(CH_2)_2AsPh_2$, ffars = $(AsMe_2)C=C(AsMe_2)CF_2CF_2$, pdma = 1,2-$(AsMe_2)_2C_6H_4$.

Results and discussion

Until recently it was thought that monodentate Group 15 ligands would replace only up to three CO groups in $Ru_3(CO)_{12}$, reactions involving ligand/metal ratios greater than 1/1 giving $Ru_3(CO)_9(L)_3$, or if harsh conditions were used, either cluster breakdown or intramolecular fragmentation reactions of the coordinated phosphine or arsine. However, we have now found that heating mixtures containing $Ru_3(CO)_{12}$ and a four- to seven-fold excess of a tertiary phosphite for short times (< 1 h) in octane afforded moderate to good yields of the tetra-substituted complexes. Similar complexes containing the ligands PMe_2R ($R = CH_2Ph$, Ph) or $P(OEt)_3$ were best obtained by heating mixtures of $Ru_3(CO)_2$ and the Group 15 ligand in the presence of sodium diphenyl ketyl in tetrahydrofuran.

Thus, brief heating of $Ru_3(CO)_{12}$ and $P(OR)_3$ ($R = Me$, Ph, or CH_2CF_3) or $P(OCH_2)_3CEt$ afforded $Ru_3(CO)_8\{P(OR)_3\}_4$ in 56–96% yields; in the latter instance, the complex was precipitated in quantitative yield as an orange powder. The electron-transfer-catalysed reaction with $P(OEt)_3$ afforded $Ru_3(CO)_{12-n}\{P(OEt)_3\}_n$ ($n = 3$, 4) in ca. 15% yields; the two complexes were readily separated by chromatography on silica gel. The tetrasubstituted tertiary phosphite complexes were obtained as red-orange powders or crystals which were characterised by elemental microanalysis and from their spectroscopic properties. The IR $\nu(CO)$ spectra contained a broad, poorly resolved absorption containing several shoulders; the maxima were between 1975–2000 cm^{-1}. In contrast with complex 4i-Ru [8], none of the complexes exhibited any bands in the bridging carbonyl region. Their fast-atom bombardment mass spectra (FAB MS) were readily obtained, and showed $[M]^+$, $[M - nCO]^+$ and $[M - nCO - P(OR)_3]^+$ ions.

The reaction between $Ru_3(CO)_{12}$ and $PMe_2(CH_2Ph)$ was described earlier [34] and afforded $Ru_3(CO)_9\{PMe_2(CH_2Ph)\}_3$ in 44% yield. Using a large excess of the tertiary phosphine, we obtained evidence (IR $\nu(CO)$ and TLC) for the formation of $Ru_3(CO)_8\{PMe_2(CH_2Ph)\}_4$ (4g-Ru), but in refluxing octane, the maximum yield was obtained after only five minutes, after which a rapid lightening of colour indicated cluster degradation had occurred to give mononuclear products. TLC examination of the solution showed that a number of white complexes had formed; these have not yet been characterised. This result is not surprising, as one of the effects of progressively introducing more tertiary phosphine ligands into a M_3 cluster is gradually to weaken the metal–metal bonds [20,21]. Complex 4g-Ru proved to be unstable on chromatography, and a pure sample was not obtained.

The other tertiary phosphine examined was PMe_2Ph. Tri- and tetra-substituted complexes 3e-Ru and 4e-Ru were obtained in 30 and 6% yields, respectively, after heating a mixture of $Ru_3(CO)_{12}$ and PMe_2Ph in refluxing tetrahydrofuran for 5 h. The two complexes were readily separated by chromatography, and formed orange (3e-Ru) and deep purple crystals (4e-Ru).

We have limited our studies to the above examples, but there seems to be no reason why other tetrasubstituted complexes containing sterically less-demanding ligands should not be obtained in the future.

Complexes containing $P(OCH_2CF_3)_3$. In Part A [1], we described the ETC reaction between $Ru_3(CO)_{12}$ and the fluorinated phosphite $P(OCH_2CF_3)_3$, which contrary to expectation, afforded all three complexes 1l-Ru, 2l-Ru and 3l-Ru. The thermal reaction described above affords 4l-Ru in reasonable yield. The structural

studies suggest that the properties of this ligand are not a straightforward extrapolation of those of $P(OEt)_3$. Thus, the short Ru–P distances found (ca. 2.25 Å) suggest a cone angle much smaller than $110°$ (based on that for $P(OEt)_3$, which has Ru–P 2.29 Å in **4k-Ru**); presumably the presence of the CF_3 groups encourages a degree of back-bonding to the P atom, thus stabilising the poly-substituted complexes. Comparison of $\nu(CO)$ for the $P(OEt)_3$ and $P(OCH_2CF_3)_3$ complexes shows that comparable $\nu(CO)$ absorptions are ca. 35 cm^{-1} higher in complex **4l-Ru** compared with complex **4k-Ru**, confirming that the fluorinated ligand is a much better electron-acceptor than triethyl phosphite, in agreement with the structural results. The FAB mass spectra of the fluorophosphite-substituted clusters contain abundant molecular ions which exhibit complex fragmentation patterns associated with breakdown of the phosphite ligands as well as the usual loss of CO groups.
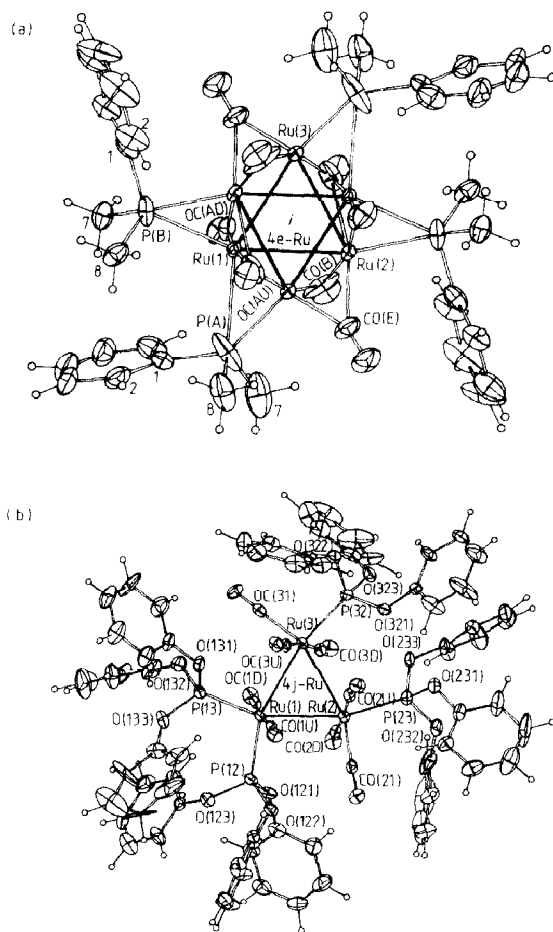
Fig. 1. Molecular projections perpendicular to the Ru_3 plane of the four complexes whose structures are recorded in the present study. 20% probability amplitudes are given for the non-hydrogen atoms, with labelling. Hydrogen atoms have arbitrary radii of 0.1 Å. (a) $Ru_3(CO)_8(PMe_2Ph)_4$ (**4e-Ru**); (b) $Ru_3(CO)_8\{P(OPh)_3\}_4$ (**4j-Ru**); (c) $Ru_3(CO)_8\{P(OEt)_3\}_4$ (**4k-Ru**); (d) $Ru_3(CO)_8\{P(OMe)_3\}_4$ (**4m-Ru**). In (a) the two components (50/50 populations) of the disordered Ru_3 core are shown together within the array of ligands; in (c) where a similar situation obtains they are deconvoluted into independent molecules.
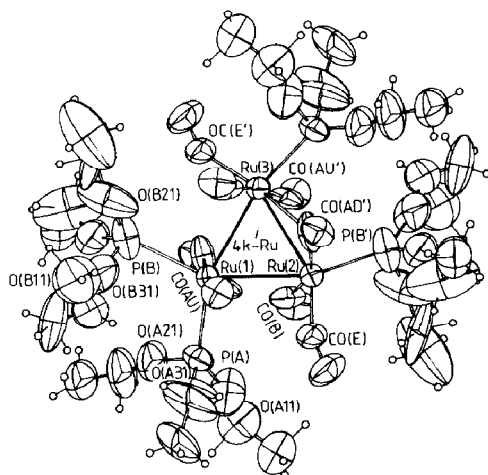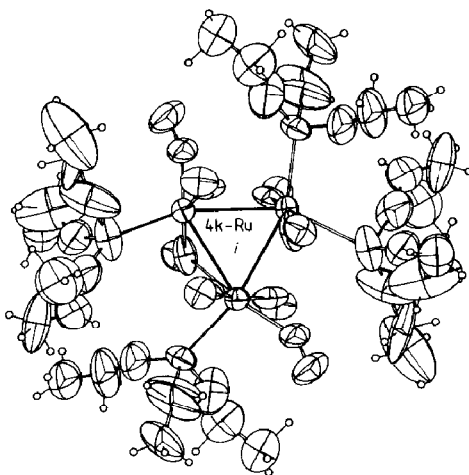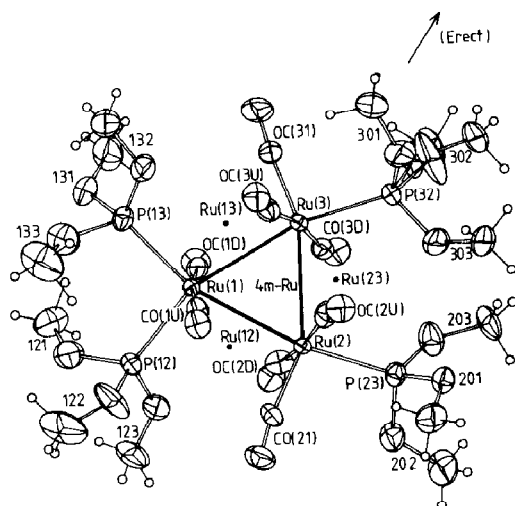
Fig. 1 (continued)

Table 1

Important bond distances (Å) in $Ru_3(CO)_8(L)_4$
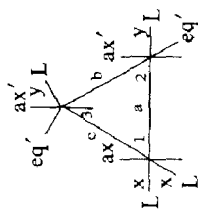
L	No.	Cone angle[a]	Ru—Ru			Ru—L[b]		Ru—CO[b]			Ref.
			a	b	c	x	y	ax	ax'	eq'	
CO	**1a-Ru**	~95	2.852(1)	2.851(1)	2.860(1)			1.942(4)		1.921(5)	22
PMe$_2$Ph	**4e-Ru**	122	2.883(3)	2.843(3)	2.872(3)	2.631(8), 2.470(4)	2.32(4), 2.187(7)	1.91	2.06	1.99	c
PPh(OMe)$_2$	**4i-Ru**	115	2.879(1)	2.797(1)	2.879(1)	2.265(2), 2.270(2)	2.277(2), 2.281(2)	1.92	2.063[d], 2.394	1.887[e], 1.918	8
P(OMe)$_3$	**4m-Ru**	107	2.865(2)	2.848(2)	2.857(1)	2.269(4), 2.271(4)	2.261(4), 2.254(4)	1.90	1.94	1.88	c
P(OEt)$_3$	**4k-Ru**	109	2.857(4)	2.855(4)	2.852(4)	2.277(8), 2.546(13)	2.21(1), 2.298(8)	1.90	2.07	1.91	c
P(OPh)$_3$	**4j-Ru**	128	2.872(2)	2.887(2)	2.870(2)	2.253(4), 2.250(4)	2.259(3), 2.270(4)	1.91	1.93	1.89	c

[a] From ref. 17. [b] Average values. [c] This work. [d] Average values for asymmetric μ-CO groups. [e] Values for terminal CO groups.

General structural considerations. The molecular structures of the four complexes are shown in Fig. 1. Table 1 summarises important bond lengths found for these complexes and for $Ru_3(\mu\text{-}CO)_2(CO)_6\{PPh(OMe)_2\}_4$ **(4i-Ru)**, reported earlier; relevant data for $Ru_3(CO)_{12}$ [22] are also included. The Ru_3 triangular core is common to each structure but, unlike the structure of **4i-Ru** which is unusual in having the $Fe_3(CO)_{12}$-type structure, the present derivatives have all four non-CO ligands coordinated in the equatorial plane of the $Ru_3(CO)_{12}$-type structure; two are coordianted to one of the ruthenium atoms (Ru(1)) and the others bonded one each to Ru(2) and Ru(3), directed away from Ru(1), in an array of incipient *mm* core symmetry.

In **4j-Ru** and **4m-Ru**, one molecule with no crystallographically imposed internal symmetry comprises the asymmetric unit of the structure; some disorder is observed in the Ru_3 core of **4m-Ru** (15.4(1)%), without any serious consequences for the precision of the determination; in addition two substituent groups of one of the phosphite ligands are also disordered. In **4e-Ru** and **4k-Ru**, one-half of the molecule comprises the asymmetric unit of the structure, a crystallographic inversion centre being located at the centre of the Ru_3 triangle. As is frequently found in structures of this type, although Ru–Ru distances are in the vicinity of the expected values, disorder of the ligating atoms is accommodated within their thermal envelopes with considerable concomitant perversion of associated geometries; this may or may not be obvious and should always be borne in mind in dealing with the parameters of such structures. In particular, in the present context, the nature of groups such as CO(AD) in **4k-Ru** as bridging or otherwise, must remain a matter of conjecture, perhaps to be resolved by future low-temperature studies. The association of "bridging" CO groups with "disorder" in **4e-Ru** and **4k-Ru** raises the question as to what extent the assignment of a CO as bridging is consequent upon the disorder model, and if real, to what extent it is instrumental in precipitating 'disorder'.

Table 2

Torsion angles (deg) in complexes $Ru_3(CO)_8(L)_4$

L	Torsion angle (deg) [a]		
	C(1)–Ru(1)–Ru(2)–C(2)	C(2)–Ru(2)–Ru(3)–C(3)	C(3)–Ru(3)–Ru(1)–C(1)
$P(OMe)_3$	33.6, 35.0	32.9, 39.3	32.0, 40.1
$P(OPh)_3$	33.2, 28.1	32.3, 28.2	29.1, 30.4
$PPh(OMe)_2$ [b]	4.6, 6.9	42.1, 49.6	49.2, 39.2
PMe_2Ph	41, 42	44, 39	44, 43
$P(OEt)_3$	44, 38	41, 39	41, 43
$Os_3\{P(OMe)_3\}_6$ [c]	30, 19	–	–

[a] Two values given, for C(nU)–Ru(n)–Ru($n+1$)–C($n+1$U), C(nD)–Ru(n)–Ru($n+1$)–C($n+1$D), respectively; signs are adapted to a common chirality. [b] Ref. 8. [c] Ref. 19.

Table 3

Average M–M and M–L bond lengths (Å) in complexes M$_3$(CO)$_{12-n}$(L)$_n$ [a]

L	Conc angle (deg)	M–M				M–L			
		$n=1$	2	3	4	1	2	3	4
M = Ru									
CO	95	2.854							
P(OCH$_2$)$_3$CEt	101	2.842				2.238			
P(OMe)$_3$	107		2.850		2.857		2.298		2.258
P(OEt)$_3$	109			2.855	2.855			2.292	2.25
P(OCH$_2$CF$_3$)$_3$	110	2.856	2.846	2.858		2.254	2.250	2.246	
PPh(OMe)$_2$	115	2.859	2.864	2.886	2.852 [b]	2.287	2.297	2.284	2.279
				2.886				2.279	
				2.881				2.278	
				2.880				2.299	
PMe$_3$	118			2.859				2.330	
PMe$_2$(CH$_2$Ph)	120			2.860				2.314	
PMe$_2$Ph	127			2.858	2.866			2.334	2.257
P(OPh)$_3$	128				2.876				2.265
PPh$_3$	145	2.886	2.842			2.380	2.357		
		2.882					2.380		
PCy$_3$	179	2.880				2.425			
		2.890				2.430			
AsMe$_2$Ph	125			2.845				2.444	
				2.844				2.446	
AsPh$_3$	142	2.868				2.464			
M = Os									
CO	95	2.877							
P(OMe)$_3$	107	2.897	2.882		2.927 [c]	2.285	2.281		2.237 [c]
			2.887				2.291		
PPh(OMe)$_2$	115	2.883	2.890			2.288	2.294		
PPh$_3$	145	2.898	2.896	2.910		2.370	2.362	2.35	
			2.905				2.358		
PBu$^t_2$(NH$_2$)	165	2.911				2.376			
		2.902				2.399			
PPh$_2$(NHPh) [d]	135	2.866				2.301			
(AsBu$^t_2$N–)$_2$S	160	2.905				2.488			

[a] See ref. 1–3 and this work. [b] M(μ-CO)$_2$M 2.797, M–M 2.879 Å [c] Values for Os$_3$(CO)$_6${P(OMe)$_3$}$_6$ from ref. 19. [d] Ref. 42.

The ligand dispositions are of interest: in **4j-Ru** and **4m-Ru**, both molecules deviate, particularly in respect of carbonyl and ligand substituent dispositions, from the idealized *mm* symmetry associated with a substituted D_{3h} carbonyl parent; these deviations are such, however, that overall molecular symmetry is not unreasonably described as *pseudo*-2, the axis passing through Ru(1) and the mid-point of Ru(2)–Ru(3). All ligands in both compounds have one substituent directed inward toward the vertical "mirror" and the other pair of substituents directed ouward. This disposition is also observed in **4k-Ru**, but not **4e-Ru**; in the latter, substituent dispositions are chiral in aspect.

Metal–metal bonds. The Ru(2)–Ru(3) separation is the shortest of the three Ru–Ru bonds in **4e-Ru**, **4i-Ru** and **4m-Ru**, and the longest in **4j-Ru**; all three distances are essentially equal in **4k-Ru**. Only in **4i-Ru**, studied earlier [8], is this bond bridged by CO groups. There is no obvious correlation with the bulk of the Group 15 ligand.

Metal–ligand separations. An inverse trend is found in the Ru–P distances: in **4j-Ru**, the distance at Ru(3) (2.270(4) Å) is perhaps slightly longer than the others (mean: 2.258 Å), with no credible difference between the two distances to Ru(1) and the other two; in **4m-Ru**, the mean is 2.70 Å, with Ru(1)–P distances perhaps slightly longer than the other two. These variations may relate to the packing (intermeshing) of substituents on the P atoms attached to Ru(1). In general, the Ru(2)–P and Ru(3)–P distances are somewhat shorter than those found in the other substituted complexes, and do not appear to be as closely related to the cone angles. These values (2.25–2.28 Å) are the shortest found in the series of cluster complexes studied, suggesting that in these complexes the greatest degree of back-bonding into the Group 15 ligand is found.

Metal–CO geometries. As found previously, the $M-CO_{eq}$ distances are shorter than the $M-CO_{ax}$ separations; of the latter, those attached to Ru(1) are shorter than those on the other two rutheniums, presumably reflecting a degree of increased back-bonding resulting from the presence of two Group 15 ligands attached to the same metal atom.

Considering the interactions between equatorial ligands as indicated by the angles at the metal atoms in **4j,k,m-Ru** there is relatively little difference between P(12)–Ru(1)–P(13) (ranging from 99.4 (**4m-Ru**) to 110.7° (**4k-Ru**)), and C(n1)–Ru(n)–P(23) (or P(32)) (98.6 (**4j-Ru**) to 111.1° (**4k-Ru**)), all values lying well above 90°, as might be expected. Angles Ru–Ru–P range from 92.2 to 102.3° and Ru–Ru–CO from 89.2–98.6° for the *cis*-OC–Ru–Ru–P moieties, while for *cis*-P–Ru–Ru–P, angles Ru–Ru–P range from 101.3 to 108.8°. These differences are not large and reflect the relatively small changes in cone angles of the tertiary phosphite ligands.

In complexes **4e-Ru** and **4k-Ru** (in particular, see the deconvoluted projection of the latter), there appear to be CO groups bridging two metal atoms. In the former, CO(AU) bridges one edge of one disordered Ru_3 component, while the symmetry-related CO ligand bridges the corresponding edge of the other disordered Ru_3 component. In addition, CO(AD), CO(B) and CO(E) occupy positions between the three pairs of partially occupied Ru sites. In **4k-Ru**, CO(AD′) bridges Ru(2) and Ru(3) at distances of 2.14(1), 2.67(2) Å respectively, while significant bending found in CO(E) (Ru(2)–C(E)–O(E), 155(1), Ru(3)–C(E′)–O(E′), 152(1)°) indicates that these ligands are semi-bridging.

Torsion angles. Table 2 lists the torsion angles calculated for the 'up' (U) and 'down' (D) axial CO ligands on adjacent metal atoms about the vector joining the two metal atoms. The angles are a measure of the distortion of the M_3L_{12} molecule from the D_{3h} symmetry found in $Ru_3(CO)_{12}$ to D_3 symmetry by twisting of the ML_4 moieties relative to one another about the Ru–Ru vectors to relieve steric interactions resulting from the introduction of the Group 15 ligands. In $Os_3(CO)_6$-$\{P(OMe)_3\}_6$, where the six tertiary phosphite ligands occupy the six equatorial sites, twisting of the $Os(CO)_2\{P(OMe)_3\}_2$ moieties results in exact D_3 symmetry [19]. The disordered aggregate has $\bar{3}$ symmetry, while the isolated molecule has only **3**
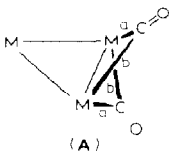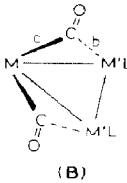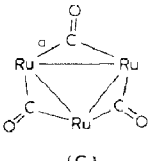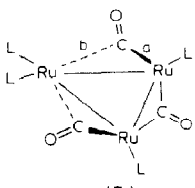
symmetry [19]. These findings accord with Lauher's predictions using a surface force field model [23].

Bridging carbonyl groups. Structural studies of a multitude of polynuclear complexes containing carbonyl groups, backed up by detailed quantitative analyses, have established the correctness of Cotton's suggestion that there is a smooth continuum which encompasses terminal, bent semi-bridging and symmetrically bridging CO groups [24]. The elegant analysis by Crabtree and Lavin [25] shows that the variations in structural parameters can be accommodated by the premise that individual examples lie on the trajectory for terminal-bridge-terminal CO exchange between metal atoms. This process is well-known, having been demonstrated by variable temperature NMR studies in solution [26] and more recently in the solid state by NMR [27] and X-ray methods [28].

The distribution of bridging and semi-bridging CO groups in $M_3(CO)_{12-n}(L)_n$ complexes results in several structural types, represented as **A**–**D**. Some examples found in the present study, together with relevant structural parameters, are listed in Table 4. The major features of the different types follow:

(i) Type A. This is the well-known $Fe_3(\mu\text{-}CO)_2(CO)_{10}$ structure, also found in many of its derivatives, and in $Ru_3(\mu\text{-}CO)_2(CO)_6\{PPh(OMe)_2\}_4$, the sole example

Table 4

Binuclear interactions of CO in $M_3(CO)_{12-n}(L)_n$ complexes

	a	b
$Fe_3(\mu\text{-}CO)_2(CO)_{10}$	1.95	2.16
$Ru_3(\mu\text{-}CO)_2(CO)_6\{PPh(OMe)_2\}_4$	2.063	2.394
(A)		
$FeRu_2(CO)_{10}(PPh_3)_2$	1.82	2.52
$Fe_3(CO)_{10}(pdma)$	1.80	2.23
$Ru_3(CO)_{10}(PPh_3)_2$	~1.9	~2.7
$Ru_3(CO)_{10}\{P(OMe)_3\}_2$	~1.9	~3.0
(B)		
$Ru_3(\mu\text{-}CO)_3(CO)_7(\mu\text{-}C_4H_4N_2)$	2.22	
(C)		
$Ru_3(CO)_8\{P(OEt)_3\}_4$	~2.0	~3.0
$Ru_3(CO)_8(PMe_2Ph)_4$	~2.0	~3.0
(D)		

of a ruthenium-containing complex with this arrangement [8]. The complexes $Fe_3(\mu\text{-}CNCF_3)(\mu\text{-}CO)(CO)_{10}$ [29] and $Os_3(\mu\text{-}CH_2)(\mu\text{-}CO)(CO)_{10}$ [30] have related structures, with one of the μ-CO groups replaced by $CNCF_3$ or CH_2 groups, respectively.

(ii) Type B. Complexes in which two of the axial CO groups attached to the unsubstituted metal atom bend towards each of the adjacent metal atoms in a manner related with the previously mentioned $D_{3h} \rightarrow D_3$ distortion. While it is true that any degree of twisting creates some degree of binuclear interaction with the appropriate CO groups as they are brought closer to the adjacent metal atoms, the effect seems to be emphasised when strong σ-donor ligands are present. This is presumably because of the electron-accepting ability of the CO π^* orbital which serves to remove excess charge from the substituted metal atom. First reported for $Fe_3(CO)_{10}(pdma)$ [31], this type of unsymmetrical bridging CO system was later found in the heterometallic cluster $FeRu_2(CO)_{10}(PPh_3)_2$ [32], and to a small degree in $Ru_3(CO)_{10}(L)_2$ (L = PPh_3 (molecule 1) [2,33], $P(OMe)_3$ [34]), in **2b-Os** (molecule 1), and possibly also for CO(3U) in **2i-Os** and **2l-Ru** [2].

(iii) Type C. The only example of a complex of this type containing each M–M bond bridged by a CO group is $Ru_3(\mu\text{-}C_4H_4N_2)(\mu\text{-}CO)_3(CO)_7$ [35]; three semi-bridging CO ligands are present in $Ru_3(CO)_9\{(PBu_2)_3SiMe\}$ [36].

(iv) Type D. Two examples **4e-Ru**, **4k-Ru** of this type of structure have been found among the tetra-substituted complexes described above. The situation is best seen in the deconvoluted picture of **4k-Ru**, where CO(AD$'$) bridges the Ru(2)–Ru(3) vector, and is terminally bonded to Ru(1$'$) located between them. This results in an electronic imbalance, with Ru(2) having three, and Ru(3) four, terminal ligands. Closer inspection shows marked bending (150–163°) of the Ru–C(B)–O(B) and Ru–C(E)–O(E) groups, allowing an appropriate redistribution of electron density. As mentioned above, the $D_{3h} \rightarrow D_3$ twisting brings some CO groups into semi-bridging locations; as a final point, we note that whereas the thermal ellipsoid of C(AD$'$) is considerably elongated, it is the oxygen atom ellipsoids of O(B), O(E), which are elongated, suggesting disorder such that O(AD$'$), or C(B), C(E), respectively, exhibit little relative positional change in the two disordered structures.

However, there is a degree of ambiguity in the interpretation of these results. In **3k-Ru**, we attribute the significant bending observed in the Ru–C–O moieties (all are < 170°) to the presence of the disordered component (75/25), so that the light atom positions, particularly C, are weighted toward an apparent semi-bridging position. A similar distortion exists with **4e-Ru**, as is clearly shown in Fig. 1(a), where all donor atoms (C or P) appear to bridge the disordered metal atom pairs, and the Ru-C-O groups are bent (147–164°).

In our examples, the presence of semi-bridging CO groups may be a further manifestation of the electronic effects of the non-CO ligands, although we have not been able to rationalise the amount of semi-bridging character in terms of the usual factors which are used to gauge the electronic effects of ligands [ν(CO) values, basicity, etc.]. Certainly we find that poly-substitution results in an increased tendency for the formation of bridging CO groups. In only one case does this result in a change from the all-terminal $M_3(CO)_{12}$ structure to that of the $M_3(\mu\text{-}CO)_2(CO)_{10}$-type, namely for L = $PPh(OMe)_2$ in the tetrasubstituted example [8]. As described above, all other $Ru_3(CO)_8(L)_4$ complexes that we have studied retain the non-bridged structure, albeit with some semi-bridging CO groups. It is likely

that just as the occurrence of terminal, semi-bridging and bridging CO groups can be related to CO exchange in binuclear complexes [25], so the various configurations found in the present and related studies of M_3L_{12} complexes relate to a continuum of movement of the M_3 core within the peripheral atom polyhedron.

The disorder phenomenon

At this time, there remain several unanswered questions concerning the nature of the disorder observed with cluster carbonyls and their derivatives. We note the recent communication [31] explaining the solid-state fluxional behaviour observed with $Fe_3(CO)_{12}$ and $Co_4(CO)_{12}$ in terms of small low energy librations of the metal polyhedron and CO envelope; convincing arguments that the 'breathing' of the latter which would be necessary for rotation of the enclosed Fe_3 core would have a higher activation energy than found in solution were advanced. The conclusion is that the crystallographic disorder arises from statistical occupation of the two orientations of the metal core within the ligand polyhedron.

In several similar structures reported here and elsewhere, we have observed similar 50/50 disorder of the metal core; examples are $Ru_3(CO)_{10}(CNBu^t)_2$, **2m-Ru** and **2m-Os, 4e-Ru** and **4k-Ru**. Invariably these have contained two or four Group 14 or 15 ligands with statistical occupation of two orientations, the ligand polyhedron having the inversion symmetry required of the observed space groups.

In other cases, however, a non-stoichiometric disorder has been found, for example, **2m-Os** (molecule 1: 95/5; but molecule 2: 50/50), **3i-Ru** (molecule 1: 94/6; molecule 4; 82.5/17.5) or **3k-Ru** (75/25). The same situation was found for $Ru_3(CO)_{11}(CNBu^t)$, but structural determinations at different temperatures showed that the occupations vary with temperatures, viz. 94/6 at 133 K, 86/14 at 295 K [38]. This could indicate that the activation energy for reorientation of the Ru_3 core within the ligand polyhedron by 'breathing' is lower than for the $Fe_3(CO)_{12}$ case, perhaps by virtue of the packing of individual molecules being tighter in the latter case. The Bu^t group protrudes into the lattice, and may hold the individual molecules further apart. Similar comments can be made for the Group 15 ligand-substituted complexes mentioned above.

The observation that only two out of the four independent molecules found in the crystal of $Ru_3(CO)_9\{PPh(OMe)_2\}_3$ show this disorder phenomenon raises some interesting questions. Are the two non-disordered molecules in a static configuration because of "crystal packing forces"? How does the degree of disorder relate to the conformation of the non-CO ligands, and how is this effect transmitted to the M_3 core? Further studies of these systems are warranted, particularly of their variable temperature solid-state NMR spectra.

Summary

In this paper and the previous three parts [1–3], we have reported the X-ray structures of 23 complexes derived from $M_3(CO)_{12}$ (M = Ru or Os) and containing from one to four monodentate tertiary phosphine, phosphite or arsine ligands. Table 3 summarises the M–M and M–P (or As) bond lengths found for these complexes together with those in the few other examples in the earlier literature. An unfortunate feature of this survey is our lack of success in obtaining X-ray quality crystals of complexes containing increasing substitution by the same ligand, except in the

case of $L = PPh(OMe)_2$, and the uncertainty of some geometrical parameters introduced by disorder in certain cases. However, trends across the series are apparent and can be summarised as follows:

(i) Substitution of CO by a more bulky ligand results in the latter occupying the sterically least demanding site, which in all cases is equatorial. (It is only ligands smaller than CO, such as nitriles [39] or isonitriles [38,40] that occupy axial sites in $M_3(CO)_{12-n}(L)_n$ complexes). The two ligands in disubstituted complexes, $M_3(CO)_{10}(L)_2$, occupy positions which puts each as far as possible from the other, i.e. in transoid sites at each end of an M–M vector. In the trisubstituted derivatives, one ligand is on each metal atom and takes up a position which results in *approximate* three-fold symmetry for the $M_3(CO)_9(L)_3$ molecule: only one complex $(L = PMe_2(CH_2Ph))$ was found to have *exact* three-fold symmetry. Finally, in the tetra-substituted complexes $Ru_3(CO)_8(L)_4$ (no osmium derivatives have been studied), one metal atom must necessarily carry two ligands, which occupy the two equatorial sites; the other two are disposed in *cisoid* sites on the other two metal atoms.

(ii) As the degree of substitution increases, so does the degree of distortion from D_{3h} symmetry [found in $M_3(CO)_{12}$] to D_3 symmetry. This is achieved by a twisting of the ML_4 groups about the M–M bonds, and also relieves the inter-ligand repulsion experienced by the axial ligands (here CO groups). A greater degree of twisting is found in complexes with the shorter M–P distances (and smaller cone angles), while within any one series (L_1, L_2 or L_3) there is an expansion of the M_3 triangle as the distortion towards D_3 symmetry increases.

(iii) Introduction of the non-CO ligand results in a lengthening of the M–M bond(s). For $M_3(CO)_{11}(L)$ complexes, this is most marked for the M–M bond *cis* to the ligand, whereas for all others, there is a non-specific enlargement of the M_3 core, as revealed by the average M–M distances. There does not appear to be any well-defined lengthening of the M–M bond *trans* to the Group 15 substituent. The most likely explanation is that the M_3 core expands to accommodate the increased size of the ligand polyhedron.

(iv) In general, we find that the average M–M distances increase with increasing degree of substitution, except in the case of $Ru_3(\mu\text{-CO})_2(CO)_6\{PPh(OMe)_2\}_4$, where there is a change in structure type. However, the observed increases are small and trends are negated by the observation of significantly different M–M distances in independent molecules (where these are found).

(v) The M–L distances for a given ligand are essentially the same throughout a series of polysubstituted complexes, and overall are a consequence of the bulk of the ligand, as measured by the cone angle [41]. It has been suggested [19] that the short Os–P distances in $Os_3(CO)_6\{P(OMe)_3\}_6$ (2.229(6), 2.245(6) Å) may be the result of increased π-back-bonding into the P $3d$ or σ^* orbitals.

(vi) the disorder found in several complexes can be modelled satisfactorily in terms of rotation of the M_3 core within a constant peripheral atom polyhedron (p.a.p.; here defined by the O atoms of the CO groups and the P (or As) atoms of the Group 15 ligand). This rotation has been shown previously to be kinetic phenomenon [38], and in the cases where 1/1 site occupancy is not found, then the degree of disorder must reflect the difficulty of rearrangement of the core within the ligand atom polyhedron.

Experimental

General conditions. All reactions were carried out under nitrogen; no special precautions were taken to exclude air during work-up, since most complexes proved to be stable in air as solids, and for short times in solution.

Instruments. Perkin–Elmer 683 double-beam spectrometer, NaCl optics (IR); Bruker WP80 spectrometer (^{1}H NMR at 80 MHz, ^{13}C NMR at 20.1 MHz). FAB mass spectra were obtained on a VG ZAB 2HF instrument equipped with a FAB source. Argon was used as the exciting gas, with source pressures typically 10^{-6} mbar; the FAB gun voltage was 7.5 kV, current 1 mA. The ion accelerating potential was 8 kV. The matrix was 3-nitrobenzyl alcohol. The complexes were made up as ca. 0.5 M solutions in acetone or dichloromethane; a drop was added to a drop of matrix and the mixture was applied to the FAB probe tip.

Starting materials. $Ru_3(CO)_{12}$ was made by a literature method [40]. The tertiary phosphines and phosphites were commercial products and were used as received. The synthesis of $Ru_3(CO)_8\{P(OEt)_3\}_4$ was described in Part C [3].

Syntheses of $Ru_3(CO)_8(L)_4$

(i) $Ru_3(CO)_8\{P(OMe)_3\}_4$. A mixture of $Ru_3(CO)_{12}$ (200 mg, 0.31 mmol) and $P(OMe)_3$ (233 mg, 1.88 mmol) was heated in refluxing deoxygenated octane (25 ml) for 30 min. Monitoring by TLC showed the formation of a trace amount of $Ru_3(CO)_9\{P(OMe)_3\}_3$ and a major, red product. The mixture was kept at room temperature overnight, when a red crystalline compound separated from solution. This compound was collected on a sintered glass filter, washed with hexane (3 × 5 ml) and dried in vacuo to yield $Ru_3(CO)_8\{P(OMe)_3\}_4$ **(4m-Ru)** (280 mg, 87%) m.p. 160 °C. Found: C, 23.48; H, 3.67. $C_{20}H_{36}O_{20}P_4Ru_3$ calcd.: C, 23.47; H, 3.54%. Infrared: $\nu(CO)$ 1990s(sh), 1975vs cm^{-1}; ^{1}H NMR: δ (CDCl$_3$) 3.61 (m, OCH_3).

(ii) $Ru_3(CO)_8\{P(OCH_2CF_3)_3\}_4$. $Ru_3(CO)_{12}$ (200 mg, 0.31 mmol) was dissolved in n-octane (50 ml), $P(OCH_2CF_3)_3$ (510 mg, 1.55 mmol) was added, and the mixture was heated for 30 min at reflux point. After cooling, the red crystalline product was collected and washed with petroleum spirit and dried giving $Ru_3(CO)_8\{P(OCH_2CF_3)_3\}_4$ **(4l-Ru)** (317 mg, 56%), m.p. 129–130 °C. Found: C, 20.79; H, 1.38%. M (FAB MS), 1841. $C_{32}H_{24}F_{36}O_{20}P_4Ru_3$, calcd.: C, 20.89; H, 1.31%; M, 1841. Infrared (CH$_2$Cl$_2$): $\nu(CO)$ 2069vw, 2019(sh), 2007vs cm^{-1}. ^{1}H NMR: δ (acetone-d_6) 4.68 (m, CH$_2$).

(iii) $Ru_3(CO)_8\{P(OCH_2)_3CEt\}_4$. To a solution of $Ru_3(CO)_{12}$ (200 mg, 0.31 mmol) in n-octane (50 ml) was added $P(OCH_2)_3CEt$ (251 mg, 0.155 mmol). After 25 min a clear solution was obtained over an orange precipitate. This was filtered off, washed with light petroleum and dried (350 mg, 96%). Although satisfactory analyses could not be obtained, this complex has spectroscopic properties suggesting it is $Ru_3(CO)_8\{POCH_2)_3CEt\}_4$ **(4n-Ru)**, m.p. 140 °C (dec). Infrared (CH$_2$Cl$_2$): $\nu(CO)$ 2059w, 2006(sh), 1988vs cm^{-1}. FAB MS: found M, 1177, calcd. 1177. ^{1}H NMR: δ (CDCl$_3$) 4.15 (m, 6H, OCH$_2$); 1.14–0.84 (m, 5H, Et).

(iv) $Ru_3(CO)_8\{P(OPh)_3\}_4$. A mixture of $Ru_3(CO)_{12}$ (200 mg, 0.31 mmol) and $P(OPh)_3$ (583 mg, 1.88 mmol) was heated in refluxing cyclohexane (30 ml) for 3 min. The product precipitated as an orange powder, which was filtered off, washed with light petroleum (3 × 10 ml) and dried (0.1 mm Hg) to give $Ru_3(CO)_8\{P(OPh)_3\}_4$ **(4j-Ru)** (495 mg, 90%), m.p. 147 °C (dec.). Found: C, 54.00; H, 3.41%; M (FAB

MS), 1769. $C_{80}H_{60}O_{20}P_4Ru_3$ calcd: C, 54.34; H, 3.42%; M, 1769. IR (CH_2Cl_2): ν(CO) 2054w, 2003(sh), 1990s; (nujol) 2060w, 2005s, 1978s(br), 1953m, 1943m cm^{-1}. ^{1}H NMR: δ (CDCl$_3$) 7.1 (m, Ph).

(v) $Ru_3(CO)_9(PMe_2Ph)_4$. To a solution of $Ru_3(CO)_{12}$ (100 mg, 0.15 mmol) in thf (30 ml) was added PMe$_2$Ph (154 mg, 1.11 mmol). After 5.5 h reflux the deep red solution was cooled and the solvent removed under reduced pressure. The residue was chromatographed by TLC (petroleum spirit/CH_2Cl_2/Et_2O, 6/1/1); an orange band (R_f 0.75) was crystallized (CH_2Cl_2/MeOH) giving large orange crystals of $Ru_3(CO)_9(PMe_2Ph)_3$ (3e-Ru) (47 mg, 30%) m.p. 139–140°C. Found: C, 40.77; H, 3.44%; M (FAB MS), 971. $C_{33}H_{33}O_9P_3Ru_3$ calcd.: C, 40.87; H, 3.43%; M, 971). Infrared (cyclohexane): ν(CO) 2039vw, 1976s, 1968s, 1941(sh) cm^{-1}. ^{1}H NMR: δ (CDCl$_3$) 7.5–7.2 (m, 5H, Ph); 1.81 (d, J 9 Hz, 6H, CH$_3$). The following band (purple, R_f 0.67) was quickly removed from the plate and crystallized (Et$_2$O/ hexane) yielding deep purple crystals of $Ru_3(CO)_8(PMe_2Ph)_4$ (4e-Ru) (11 mg, 6%), m.p. 133–134°C. Found: C, 44.50; H, 4.14%; M (FAB MS) 1081. $C_{40}H_{44}O_8P_4Ru_3$ calcd.: C, 44.49; H, 4.11%; M, 1081. Infrared (cyclohexane): ν(CO) 2019w, 1980(sh), 1969s, 1952s, 1938(sh) cm^{-1}. ^{1}H NMR: δ (CD$_2$Cl$_2$) 7.4–7.1 (m, 5H, Ph); 1.71 (d, J 8 Hz, CH$_3$); 1.30 (d, J 8 Hz, CH$_3$).

(vi) $Ru_3(CO)_8\{PMe_2(CH_2Ph)\}_4$. Thermal reaction of a large excess (7/1) of the phosphine resulted in the formation of the tetra-substituted cluster. This was readily observed by TLC (petroleum spirit/CH_2Cl_2, 1/1) as a purple band (R_f 0.48) following the orange band (R_f 0.60) of the tri-substituted product. In thf the tetra-substituted product was observed during 8.5 h reflux but yields could not be optimised and the product was found unstable with respect to TLC. When carried out in refluxing n-octane the reaction contains a maximum of the tetra-substituted complex after 5 min reflux, after which rapid lightening of colour is observed as cluster degradation occurred to give colourless mononuclear products (TLC).

Crystallography. Data sets were obtained with four-circle diffractometers, and application of absorption corrections and the refinements were carried out as described in Part A [1]. The molecular plots and atom numbering for 4j,m-Ru follow the scheme previously used: the Group 15 ligands always occupy the sites of CO(12), CO(13), CO(23) and CO(32); for 4e,k-Ru with 50% disorder, so that each ligand is associated with two ruthenium atoms, labelling is as shown on the Figures. Non-hydrogen atom coordinates and relevant metal environment data are given in for 4e-Ru in Tables 5 and 9, for 4j-Ru in Tables 6 and 10, for 4k-Ru in Tables 7 and 11 and for 4m-Ru in Tables 8 and 12.

Crystal data. $Ru_3(CO)_8(PMe_2Ph)_4$ (4e-Ru) = $C_{40}H_{44}O_8P_4Ru_3$, M = 1079.9, triclinic, space group $P\bar{1}$ (C_i^1, No. 2), a 12.040(2), b 10.482(6), c 9.549(4) Å, α 86.26(4), β 69.69(3), γ 78.72(3)°, U 1108.4(6) Å^3, D_c ($Z = 1$) 1.52 g cm^{-3}. $F(000) = 1080$. μ_{Mo} 10.5 cm^{-1}. Specimen: $0.22 \times 0.15 \times 0.50$ mm. $A^*_{min,max} = 1.17, 1.33$. $2\theta_{max}$ 50°. $N = 3629$, N_o (number of observed data with $I > 3\sigma(I)$) = 2056, $R = 0.076$, $R' = 0.075$ ($n = 4$).

Abnormal features. The molecule in space group $P\bar{1}$ has an Ru$_3$ core disordered about the inversion centre, any other ligand disorder being contained with the large thermal envelopes, which presumably also accounts for the high residuals.

$Ru_3(CO)_8\{P(OPh)_3\}_4$ (4j-Ru) = $C_{80}H_{60}O_{20}P_4Ru_3$, M = 1768.5, monoclinic, space group $P2_1/c$ (C_{2h}^5, No. 14), a 21.14(1), b 13.820(9), c 27.24(3) Å, β 106.34(6)°, U 7636(7) Å^3, D_c ($Z = 4$) 1.54 g cm^{-3}. $F(000) = 4848$. μ_{Mo} 6.8 cm^{-1}.

Table 5

Non-hydrogen atom coordinates (**4e-Ru**)

Atom	x	y	z
Ru(1) [a]	0.5389(2)	0.3878(2)	0.6037(2)
Ru(2) [a]	0.5684(2)	0.6190(2)	0.4229(2)
Ru(3) [a]	0.3644(2)	0.5028(2)	0.4676(2)
Ligand A			
P(A)	0.7542(6)	0.3641(5)	0.6293(5)
C(A1)	0.789(1)	0.198(1)	0.676(1)
C(A2)	0.777(1)	0.153(1)	0.817(2)
C(A3)	0.803(2)	0.017(2)	0.844(2)
C(A4)	0.836(2)	−0.065(2)	0.725(2)
C(A5)	0.851(1)	−0.028(1)	0.587(2)
C(A6)	0.823(1)	0.101(1)	0.564(2)
C(A7)	0.890(2)	0.373(2)	0.487(2)
C(A8)	0.762(2)	0.447(2)	0.784(2)
Ligand B			
P(B)	0.4285(4)	0.2284(3)	0.7654(4)
C(B1)	0.263(1)	0.227(1)	0.835(1)
C(B2)	0.188(2)	0.312(2)	0.944(2)
C(B3)	0.068(2)	0.312(2)	0.997(2)
C(B4)	0.025(1)	0.230(2)	0.941(2)
C(B5)	0.095(1)	0.140(2)	0.833(2)
C(B6)	0.222(1)	0.135(1)	0.778(2)
C(B7)	0.494(1)	0.063(1)	0.709(2)
C(B8)	0.448(1)	0.239(2)	0.941(2)
Carbonyls			
C(AU)	0.496(1)	0.522(1)	0.745(1)
O(AU)	0.4565(10)	0.5765(10)	0.8566(10)
C(AD)	0.584(1)	0.272(1)	0.442(1)
O(AD)	0.6352(8)	0.1931(8)	0.3546(10)
C(B)	0.709(1)	0.467(2)	0.313(2)
O(B)	0.7771(9)	0.4127(9)	0.2096(10)
C(E)	0.676(1)	0.668(1)	0.521(2)
O(E)	0.7221(10)	0.7323(10)	0.5539(12)

[a] Population 0.5.

Specimen: $0.12 \times 0.24 \times 0.12$ mm. $A^{\star}_{min,max} = 1.07$, 1.09. $2\theta_{max}$ $50°$. $N = 13563$, N_o ($I > 2\sigma(I)$) $= 6107$, $R = 0.073$, $R' = 0.052$ ($n = 5$).

$Ru_3(CO)_8\{P(OEt)_3\}_4$ (**4k-Ru**) $= C_{32}H_{60}O_{20}P_4Ru_3$, $M = 1191.9$, monoclinic, space group $C2/c$ (C^6_{2h}, No. 15), a 18.897(6), b 12.465(4), c 22.244(7) Å, β 102.03(4)°, U 5149(3) Å^3. D_c ($Z = 4$) 1.55 g cm^{-3}. $F(000) = 2416$. μ_{Mo} 11.3 cm^{-1}. Specimen: $0.70 \times 0.45 \times 0.17$ mm. $A^{\star}_{min,max} = 1.22$, 1.66. $2\theta_{max}$ $45°$. $N = 3260$, N_o ($I > 2\sigma(I)$) $= 1729$, $R = 0.0661$, $R' = 0.048$ ($n = 2$).

Abnormal features. The molecule in space group $C2/c$ has an Ru$_3$ core disordered about an inversion centre. With the exception of one of the terminal ligand carbon atoms, ligand disorder was not resolvable and presumably is contained within the very large thermal envelopes which presumably account also for the higher than desirable residuals. One of the carbonyl groups may be semi-bridging. In both this and the previous structure, the molecules pack in neat layers.

Table 6

Non-hydrogen atom coordinates (**4j-Ru**)

Atom	x	y	z
Ru(1)	0.79180(5)	0.22934(7)	0.53697(3)
Ru(2)	0.71337(5)	0.11309(7)	0.45485(4)
Ru(3)	0.70006(5)	0.32109(7)	0.45165(3)
P(12)	0.8323(2)	0.1085(3)	0.5924(1)
O(121)	0.7756(4)	0.0520(6)	0.6087(3)
C(1211)	0.7798(6)	−0.039(1)	0.6300(5)
C(1212)	0.7682(8)	−0.122(1)	0.5991(5)
C(1213)	0.7706(8)	−0.212(1)	0.6210(6)
C(1214)	0.7826(8)	−0.222(1)	0.6716(6)
C(1215)	0.7920(7)	−0.142(1)	0.7021(5)
C(1216)	0.7921(6)	−0.051(1)	0.6815(4)
O(122)	0.8709(4)	0.0255(6)	0.5717(3)
C(1221)	0.9344(6)	−0.0145(9)	0.5951(5)
C(1222)	0.9793(6)	0.0011(9)	0.5693(4)
C(1223)	1.0438(6)	−0.036(1)	0.5881(5)
C(1224)	1.0560(7)	−0.090(1)	0.6329(5)
C(1225)	1.0097(7)	−0.105(1)	0.6565(5)
C(1226)	0.9472(7)	−0.069(1)	0.6384(5)
O(123)	0.8877(4)	0.1280(6)	0.6466(3)
C(1231)	0.8820(6)	0.1522(8)	0.6946(4)
C(1232)	0.8341(7)	0.2074(11)	0.7023(4)
C(1233)	0.8335(8)	0.231(1)	0.7506(5)
C(1234)	0.8821(8)	0.191(1)	0.7907(5)
C(1235)	0.9335(7)	0.136(1)	0.7821(5)
C(1236)	0.9316(7)	0.115(1)	0.7331(4)
P(13)	0.8476(2)	0.3617(3)	0.5734(1)
O(131)	0.8716(4)	0.4268(6)	0.5343(3)
C(1311)	0.9010(6)	0.517(1)	0.5429(5)
C(1312)	0.8670(7)	0.598(1)	0.5385(6)
C(1313)	0.8968(9)	0.687(1)	0.5451(8)
C(1314)	0.9618(9)	0.696(1)	0.5561(6)
C(1315)	0.9963(8)	0.614(1)	0.5608(7)
C(1316)	0.9687(7)	0.522(1)	0.5552(6)
O(132)	0.8081(4)	0.4429(6)	0.5966(3)
C(1321)	0.8123(7)	0.4668(9)	0.6471(5)
C(1322)	0.7588(7)	0.458(1)	0.6633(6)
C(1323)	0.7616(9)	0.485(1)	0.7128(6)
C(1324)	0.819(1)	0.520(1)	0.7435(5)
C(1325)	0.8698(8)	0.528(2)	0.7241(6)
C(1326)	0.8670(7)	0.507(1)	0.6761(6)
O(133)	0.9107(4)	0.3594(7)	0.6219(3)
C(1331)	0.9686(6)	0.308(1)	0.6312(6)
C(1332)	1.0029(8)	0.300(2)	0.6816(7)
C(1333)	1.069(1)	0.266(2)	0.695(1)
C(1334)	1.0733(8)	0.205(1)	0.663(1)
C(1335)	1.0500(9)	0.221(1)	0.608(1)
C(1336)	0.9915(7)	0.273(1)	0.5951(8)
P(23)	0.6271(2)	0.0626(3)	0.3903(1)
O(231)	0.6366(4)	0.0542(6)	0.3338(3)
C(2311)	0.6529(6)	−0.0312(9)	0.3136(5)
C(2312)	0.7132(7)	−0.073(1)	0.3332(5)
C(2313)	0.7269(7)	−0.158(1)	0.3115(6)
C(2314)	0.6843(8)	−0.193(1)	0.2719(8)

Table 6 (continued)

Atom	x	y	z
C(2315)	0.6252(9)	− 0.152(2)	0.2496(9)
C(2316)	0.6107(7)	− 0.065(1)	0.2716(6)
O(232)	0.5931(4)	− 0.0415(6)	0.3923(3)
C(2321)	0.6020(6)	− 0.1078(9)	0.4317(5)
C(2322)	0.6509(7)	− 0.173(1)	0.4398(5)
C(2323)	0.6566(9)	−0.242(1)	0.4785(7)
C(2324)	0.611(1)	− 0.236(2)	0.5034(6)
C(2325)	0.559(1)	− 0.183(2)	0.4957(8)
C(2326)	0.5575(8)	− 0.110(1)	0.4580(6)
O(233)	0.5653(4)	0.1330(6)	0.3802(3)
C(2331)	0.5013(5)	0.1103(9)	0.3491(4)
C(2332)	0.4551(6)	0.092(1)	0.3724(5)
C(2333)	0.3932(7)	0.073(1)	0.3456(6)
C(2334)	0.3757(6)	0.073(1)	0.2953(7)
C(2335)	0.4216(7)	0.093(1)	0.2695(5)
C(2336)	0.4869(6)	0.114(1)	0.2972(5)
P(32)	0.6370(2)	0.3588(2)	0.3718(1)
O(321)	0.6416(4)	0.2820(6)	0.3297(3)
C(3211)	0.6173(6)	0.2851(9)	0.2754(4)
C(3212)	0.5642(7)	0.336(1)	0.2496(4)
C(3213)	0.5450(7)	0.330(1)	0.1962(5)
C(3214)	0.5799(9)	0.280(1)	0.1717(5)
C(3215)	0.632(1)	0.227(2)	0.1979(5)
C(3216)	0.6490(7)	0.231(1)	0.2502(5)
O(322)	0.6475(4)	0.4602(6)	0.3465(3)
C(3221)	0.7105(6)	0.5006(8)	0.3519(4)
C(3222)	0.7480(7)	0.470(1)	0.3229(5)
C(3223)	0.8088(8)	0.515(1)	0.3284(6)
C(3224)	0.8286(8)	0.589(1)	0.3632(6)
C(3225)	0.7897(8)	0.622(1)	0.3919(6)
C(3226)	0.7284(7)	0.577(1)	0.3854(5)
O(323)	0.5568(4)	0.3655(6)	0.3600(3)
C(3231)	0.5228(6)	0.427(1)	0.3845(5)
C(3232)	0.5382(8)	0.517(1)	0.3996(7)
C(3233)	0.4939(8)	0.562(2)	0.4217(7)
C(3234)	0.440(1)	0.534(2)	0.4259(7)
C(3235)	0.427(1)	0.441(2)	0.4118(9)
C(3236)	0.4675(8)	0.388(1)	0.3912(7)
C(1U)	0.8524(5)	0.2010(8)	0.4997(4)
O(1U)	0.8941(4)	0.1840(6)	0.4813(3)
C(1D)	0.7210(6)	0.2529(9)	0.5672(4)
O(1D)	0.6822(4)	0.2680(7)	0.5877(3)
C(2U)	0.7546(6)	0.1564(9)	0.4056(4)
O(2U)	0.7788(4)	0.1703(6)	0.3727(3)
C(2D)	0.6664(6)	0.0866(8)	0.5059(4)
O(2D)	0.6367(4)	0.0647(7)	0.5333(3)
C(21)	0.7639(6)	0.0012(9)	0.4671(4)
O(21)	0.7991(5)	− 0.0643(7)	0.4710(3)
C(3U)	0.7820(5)	0.3467(8)	0.4359(4)
O(3U)	0.8288(4)	0.3682(6)	0.4247(3)
C(3D)	0.6238(5)	0.2731(9)	0.4709(4)
O(3D)	0.5754(4)	0.2590(7)	0.4808(3)
C(31)	0.6979(5)	0.4437(9)	0.4835(4)
O(31)	0.6925(4)	0.5138(6)	0.5031(3)

$Ru_3(CO)_8\{P(OMe)_3\}_4$ **(4m-Ru)** $= C_{20}H_{36}O_{20}P_4Ru_3$, $M = 1023.6$, monoclinic, space group $P2_1$ (C_2^2, No. 4), a 9.821(2), b 17.384(6), c 10.912(3) Å, β 94.88(2)°, U 1856(1) Å^3. D_c ($Z = 2$) 1.83 g cm^{-3}. $F(000) = 1016$. μ_{Mo} 13.5 cm^{-1}. Specimen: $0.15 \times 0.05 \times 0.15$ mm. $A^*_{min,max} = 1.07$, 1.09 (analytical correction). $2\theta_{max} = 50°$. $N = 3261$, $N_o = 2726$, $R = 0.041$, $R' = 0.046$ ($n = 1$) (preferred chirality).

Abnormal features. Among the ligands, disorder was only observed (and refined) for one of the methoxy ligand substituents. Within the core, two components were

Table 7

Non-hydrogen atom coordinates (**4k-Ru**)

Atom	x	y	z
Ru(1) [a]	0.93250(8)	0.0176(2)	0.94176(8)
Ru(2) [a]	1.03739(10)	0.1216(1)	1.03415(9)
Ru(3) [a]	1.03065(10)	−0.1083(2)	1.03016(10)
Ligand A			
P(A)	0.8678(2)	0.1677(4)	0.9037(2)
O(A11)	0.8489(6)	0.266(1)	0.9384(7)
C(A11)	0.821(2)	0.346(2)	0.951(1)
C(A12)	0.838(1)	0.438(1)	0.971(1)
O(A21)	0.7916(7)	0.125(1)	0.8816(8)
C(A21)	0.734(1)	0.117(3)	0.871(1)
C(A22)	0.682(1)	0.087(2)	0.836(1)
O(A31)	0.880(1)	0.206(1)	0.8418(8)
C(A31)	0.907(2)	0.257(2)	0.814(2)
C(A32)	0.900(2)	0.314(2)	0.770(1)
Ligand B			
P(B)	0.8854(4)	−0.1497(7)	0.8790(3)
O(B11)	0.8121(8)	−0.184(1)	0.8872(8)
C(B11)	0.768(1)	−0.236(3)	0.890(1)
C(B12)	0.702(1)	−0.233(2)	0.904(1)
O(B21)	0.9188(10)	−0.250(2)	0.8542(9)
C(B21)	0.935(3)	−0.327(2)	0.847(2)
C(B22)	0.966(2)	−0.411(2)	0.851(2)
O(B31)	0.864(1)	−0.100(1)	0.8195(8)
C(B31) [a]	0.872(2)	−0.062(3)	0.770(5)
C(B31′) [a]	0.843(4)	−0.109(5)	0.767(6)
C(B32)	0.830(1)	−0.044(2)	0.7135(9)
Carbonyls			
C(AU)	1.0062(7)	0.055(1)	0.8970(6)
O(AU)	1.0386(5)	0.0595(8)	0.8609(4)
C(AD)	0.8780(7)	−0.038(1)	0.9964(6)
O(AD)	0.8306(4)	−0.0387(8)	1.0206(4)
C(B)	0.9398(8)	0.141(1)	1.0553(8)
O(B)	0.9028(5)	0.1657(8)	1.0850(5)
C(E)	1.0308(7)	0.2394(9)	0.9848(6)
O(E)	1.0457(6)	0.3201(7)	0.9720(5)

[a] Population: 0.5; for C(B31, B31′) associated H atoms likewise; isotropic thermal parameter refinements.

Table 8

Non-hydrogen atom coordinates (**4m-Ru**)

Atom	x	y	z
Ru(1) [a]	0.69003(9)	0	0.83211(8)
Ru(2) [a]	0.70752(11)	0.15749(6)	0.75777(9)
Ru(3) [a]	0.86645(10)	0.04328(6)	0.64877(9)
Ligand 12			
P(12)	0.5701(3)	0.0087(2)	1.0003(3)
O(121)	0.4142(9)	− 0.0080(7)	0.9950(9)
C(121)	0.3143(18)	0.0395(14)	0.9366(22)
O(122)	0.5914(13)	0.0824(6)	1.0758(10)
C(122)	0.5428(25)	0.0962(11)	1.1950(17)
O(123)	0.5919(18)	− 0.0574(9)	1.1006(9)
C(123)	0.6692(38)	− 0.0898(17)	1.1654(18)
Ligand 13			
P(13)	0.6952(4)	− 0.1300(2)	0.8117(3)
O(131)	0.5758(13)	− 0.1814(8)	0.8529(15)
C(131)	0.4437(17)	− 0.1747(12)	0.8382(20)
O(132)	0.8204(13)	− 0.1710(7)	0.8888(16)
C(132)	0.8357(31)	− 0.2364(17)	0.9469(25)
O(133)	0.6985(15)	− 0.1571(6)	0.6821(12)
C(133)	0.6899(24)	− 0.2295(10)	0.6301(22)
Ligand 23 (OC(232,232′) site occupancies 0.5) (H likewise)			
P(23)	0.7975(4)	0.2704(2)	0.7029(3)
O(231)	0.8488(17)	0.3277(7)	0.8076(15)
C(231)	0.7954(28)	0.3522(12)	0.9118(21)
O(232)	0.6696(16)	0.3121(13)	0.6147(17)
O(232′)	0.7343(24)	0.3335(16)	0.6382(35)
C(232)	0.6935(45)	0.3867(21)	0.5553(36)
C(232′)	0.6253(60)	0.3306(26)	0.5634(30)
O(233)	0.9286(12)	0.2690(7)	0.6343(12)
C(233)	1.0390(18)	0.3190(11)	0.6364(21)
Ligand 32			
P(32)	0.9519(4)	0.038(2)	0.4804(3)
O(321)	1.0889(8)	0.1405(5)	0.4906(7)
C(321)	1.2081(17)	0.1028(12)	0.5447(19)
O(322)	0.9776(13)	0.0253(6)	0.3883(9)
C(322)	1.0319(32)	0.0369(14)	0.2729(16)
O(323)	0.8618(11)	0.1506(8)	0.3994(11)
C(323)	0.8889(22)	0.2163(9)	0.3370(13)
Carbonyl groups			
C(1U)	0.5317(12)	0.0080(8)	0.7218(10)
O(1U)	0.4356(9)	0.0025(7)	0.6534(8)
C(1D)	0.8631(12)	− 0.0004(8)	0.9249(10)
O(1D)	0.9621(8)	− 0.0036(6)	0.9853(8)
C(2U)	0.6257(13)	0.1381(7)	0.5890(11)
O(2U)	0.5614(10)	0.1383(6)	0.5010(8)
C(2D)	0.7980(14)	0.1575(8)	0.9221(11)
O(2D)	0.8527(11)	0.1682(6)	1.0168(8)
C(21)	0.5397(13)	0.1928(8)	0.8057(13)
O(21)	0.4403(11)	0.2176(7)	0.8271(12)
C(3U)	0.7266(12)	− 0.0092(9)	0.5440(11)
O(3U)	0.6578(11)	− 0.0391(6)	0.4722(9)

Table 8 (continued)

Atom	x	y	z
C(3D)	0.9772(15)	0.1088(9)	0.7584(12)
O(3D)	1.0683(10)	0.1364(6)	0.8182(9)
C(31)	0.9790(14)	−0.0439(7)	0.6749(12)
O(31)	1.0577(11)	−0.0915(6)	0.6837(10)
Fractional ruthenium atoms			
Ru(12) [a]	0.6399(8)	0.0920(4)	0.8451(6)
Ru(23) [a]	0.8130(7)	0.1351(4)	0.6628(6)
Ru(31) [a]	0.7978(8)	−0.0228(4)	0.7357(6)

[a] Populations: Ru(1,2,3), 0.846(1). Ru(12,23,31), 1−0.846(1). Ru(1) defines origin.

found. They were refined with independent atom populations and constrained at the mean of 0.846, 1−0.846 in the final cycles. No further ligand fragments were observed and all concomitant disorder must be contained with the present thermal envelopes; the usual caveat is made regarding associated geometries. The chirality as found is the enantiomer of the systematic scheme.

Table 9(a)

Ruthenium environments (**4e-Ru**); numerals pertaining to phosphorus are *italicised* here and in subsequent tables

	$n = 1$	$n = 2$	$n = 3$
Distances (Å)			
Ru(n)–Ru($n+1$)	2.889(3)	2.842(3)	2.873(3)
Ru(n)–C(nU)	1.89(2)	2.02(1)	1.99(2)
Ru(n)–C(nD)	1.88(1)	2.11(1)	2.13(1)
Ru(n)–L($nn+1$)	*2.650(8)*	*2.323(4)*	1.92(2)
Ru(n)–L($nn−1$)	*2.460(4)*	2.00(2)	*2.193(6)*
Angles (degrees)			
Ru($n−1$)–Ru(n)–Ru($n+1$)	59.10(7)	60.18(7)	60.72(7)
Ru($n−1$)–Ru(n)–C(nU)	94.8(6)	94.3(3)	96.8(5)
Ru($n−1$)–Ru(n)–C(nD)	80.7(5)	71.9(4)	62.3(5)
Ru($n−1$)–Ru(n)–L($nn+1$)	*151.0(1)*	*163.0(2)*	139.7(4)
Ru($n−1$)–Ru(n)–L($nn−1$)	*99.1(1)*	91.5(4)	*106.5(2)*
Ru($n+1$)–Ru(n)–C(nU)	76.4(4)	68.3(4)	71.6(5)
Ru($n+1$)–Ru(n)–C(nD)	95.7(4)	100.8(5)	89.0(5)
Ru($n+1$)–Ru(n)–L($nn+1$)	*92.6(1)*	*106.4(2)*	86.5(5)
Ru($n+1$)–Ru(n)–L($nn−1$)	*156.5(1)*	144.7(4)	*165.5(2)*
C(nU)–Ru(n)–C(nD)	172.1(6)	165.8(6)	157.1(7)
C(nU)–Ru(n)–L($nn+1$)	*83.6(6)*	*89.5(4)*	94.0(7)
C(nU)–Ru(n)–L($nn−1$)	*98.5(4)*	95.6(6)	*105.1(5)*
C(nD)–Ru(n)–L($nn+1$)	*97.3(5)*	*102.7(5)*	96.9(5)
C(nD)–Ru(n)–L($nn−1$)	*88.7(4)*	88.4(6)	*90.6(5)*
L($nn+1$)–Ru(n)–L($nn−1$)	*109.8(2)*	*104.6(4)*	*107.9(5)*

Table 9(b)

Ruthenium environments (**4e-Ru**). r is the ruthenium–other atom distance (Å); other entries in the matrices are the angles subtended at the ruthenium by the relevant atoms at the head of the row and column.

Ru(1)

Atom	r	Ru(3)	C(AU)	C(AD)	P(A)	P(B)
Ru(2)	2.889(3)	59.10(7)	76.4(4)	95.7(4)	92.6(1)	156.5(1)
Ru(3)	2.873(3)		94.8(6)	80.7(5)	151.0(1)	99.1(1)
C(AU)	1.89(2)			172.1(5)	83.6(6)	98.5(4)
C(AD)	1.88(1)				97.3(5)	88.7(4)
P(A)	2.650(8)					109.8(2)
P(B)	2.460(4)					

Ru(1)...Ru(2′,3′) are 1.415(3), 1.734(3) Å

Ru(2)

Atom	r	Ru(1)	C(AD′)	C(B)	P(B′)	C(E)
Ru(3)	2.842(3)	60.18(7)	68.3(5)	100.8(5)	106.4(2)	144.7(4)
Ru(1)	2.889(3)		94.3(3)	71.9(4)	163.0(2)	91.5(4)
C(AD′)	2.02(1)			165.8(6)	89.5(4)	95.6(6)
C(B)	2.11(1)				102.7(5)	88.4(6)
P(B′)	2.323(4)					104.6(4)
C(E)	2.00(2)					

Ru(2)...Ru(1′,3′) are 1.415(3), 1.841(3) Å

Ru(3)

Atom	r	Ru(2)	C(B′)	C(AU′)	C(E′)	P(A′)
Ru(1)	2.873(3)	60.72(7)	71.6(5)	89.0(5)	86.5(5)	165.5(2)
Ru(2)	2.842(3)		96.8(5)	62.3(5)	139.7(4)	106.5(2)
C(B′)	1.99(2)			157.1(7)	94.0(7)	105.1(5)
C(AU′)	2.13(1)				96.9(5)	90.6(5)
C(E′)	1.93(2)					107.9(6)
P(A′)	2.193(6)					

Ru(3)...Ru(1′,2′) are 1.734(3), 1.841(3) Å

For carbonyls AU; AD; B; E, respectively: r(C—O) is 1.14(2); 1.14(1); 1.14(2); 1.07(2) Å Ru—C—O is 161(1), 147(1), Ru(1,3′); 164(1), 153(1) (Ru(1,2′)); 153(1), 153(1), (Ru(2,3′)); 155(1), 149(1)° (Ru(2,3′). Deviations δ(C) from the Ru$_3$ plane are: -1.78; 1.82; 1.83; -0.76 Å δ(P(A,B)) are 0.315, -0.402 Å.

Table 10

Ruthenium environments (**4j-Ru**)

	$n = 1$	$n = 2$	$n = 3$
Distances (Å)			
Ru(n)–Ru($n + 1$)	2.872(2)	2.887(2)	2.870(2)
Ru(n)–C(nU)	1.89(1)	1.89(1)	1.93(1)
Ru(n)–C(nD)	1.93(1)	1.96(1)	1.95(1)
Ru(n)–L($nn + 1$)	*2.253(4)*	*2.259(3)*	1.91(1)
Ru(n)–L($nn - 1$)	*2.250(4)*	1.86(1)	*2.270(4)*
Angles (degrees)			
Ru($n - 1$)–Ru(n)–Ru($n + 1$)	60.38(6)	59.77(5)	59.85(4)
Ru($n - 1$)–Ru(n)–C(nU)	93.6(3)	95.5(3)	95.9(3)
Ru($n - 1$)–Ru(n)–C(nD)	81.0(3)	81.3(3)	74.6(4)
Ru($n - 1$)–Ru(n)–L($nn + 1$)	*156.01(1)*	*160.4(1)*	152.1(3)
Ru($n - 1$)–Ru(n)–L($nn - 1$)	*98.6(1)*	98.6(3)	*106.5(1)*
Ru($n + 1$)–Ru(n)–C(nU)	78.2(3)	74.0(4)	79.4(3)
Ru($n + 1$)–Ru(n)–C(nD)	94.6(3)	98.2(3)	93.1(3)
Ru($n + 1$)–Ru(n)–L($nn + 1$)	*97.8(1)*	*103.5(1)*	96.9(3)
Ru($n + 1$)–Ru(n)–L($nn - 1$)	*156.1(1)*	151.8(4)	*163.5(1)*
C(nU)–Ru(n)–C(nD)	172.5(4)	172.1(6)	170.1(5)
C(nU)–Ru(n)–L($nn + 1$)	*91.1(3)*	*88.8(3)*	94.3(5)
C(nU)–Ru(n)–L($nn - 1$)	*93.1(3)*	92.0(6)	*93.8(3)*
C(nD)–Ru(n)–L($nn + 1$)	*91.8(3)*	*92.0(3)*	93.0(5)
C(nD)–Ru(n)–L($nn - 1$)	*92.7(3)*	95.6(5)	*91.7(3)*
L($nn + 1$)–Ru(n)–L($nn - 1$)	*104.7(1)*	*100.4(3)*	*98.6(3)*
Carbonyl distances (Å) ($\delta(C)$ is the deviation from the Ru$_3$ plane)			
C(nU)–O(nU)	1.15(2)	1.17(2)	1.15(1)
C(nD)–O(nD)	1.13(2)	1.14(2)	1.14(2)
C($nn + 1$)–O($nn + 1$)	–	1.16(2)	1.13(2)
$\delta(C(n$U$))$	−1.812	−1.743	−1.848
$\delta(C(n$D$))$	1.871	1.870	1.829
$\delta(C, P(nn + 1))$	*0.412*	*0.423*	*0.537*
$\delta(C, P(nn - 1))$	−0.463	−0.607	−0.382
Carbonyl angles (degrees)			
Ru(n)–C(nU)–O(nU)	173.5(8)	170.7(10)	174.9(9)
Ru(n)–C(nD)–O(nD)	175.8(10)	174.3(12)	169.6(11)
Ru(n)–C($nn + 1$)–O($nn + 1$)	–	–	174.9(11)
Ru(n)–C($nn - 1$)–O($nn - 1$)	–	172.4(12)	–

Table 11(a)

Ruthenium environments (**4k-Ru**)

	$n = 1$	$n = 2$	$n = 3$
Distances (Å)			
Ru(n)–Ru($n + 1$)	2.857(4)	2.869(3)	2.877(3)
Ru(n)–C(nU)	1.94(1)	2.14(1)	2.13(2)
Ru(n)–C(nD)	1.89(1)	2.02(2)	2.00(1)
Ru(n)–L($nn + 1$)	*2.301(5)*	*2.197(6)*	1.99(1)
Ru(n)–L($nn - 1$)	*2.565(9)*	1.82(1)	*2.292(5)*
Angles (degrees)			
Ru($n - 1$)–Ru(n)–Ru($n + 1$)	60.05(6)	60.31(6)	59.64(6)
Ru($n - 1$)–Ru(n)–C(nU)	92.8(4)	90.5(4)	101.4(4)
Ru($n - 1$)–Ru(n)–C(nD)	73.9(4)	71.6(4)	70.4(4)
Ru($n - 1$)–Ru(n)–L($nn + 1$)	*156.3(1)*	*160.5(3)*	147.6(4)
Ru($n - 1$)–Ru(n)–L($nn - 1$)	*91.8(2)*	89.0(4)	*106.0(1)*
Ru($n + 1$)–Ru(n)–C(nU)	77.9(4)	62.4(4)	75.3(4)
Ru($n + 1$)–Ru(n)–C(nD)	95.6(4)	95.0(4)	94.9(4)
Ru($n + 1$)–Ru(n)–L($nn + 1$)	*97.8(1)*	*101.8(3)*	93.5(4)
Ru($n + 1$)–Ru(n)–L($nn - 1$)	150.7(2)	142.1(4)	*162.5(1)*
C(nU)–Ru(n)–C(nD)	166.7(5)	156.6(6)	169.8(5)
C(nU)–Ru(n)–L($nn + 1$)	*90.2(4)*	*87.1(4)*	87.2(6)
C(nU)–Ru(n)–L($nn - 1$)	*97.0(4)*	99.3(6)	*99.7(4)*
C(nD)–Ru(n)–L($nn + 1$)	*102.4(5)*	*104.7(5)*	96.7(6)
C(nD)–Ru(n)–L($nn - 1$)	*82.8(5)*	95.4(6)	*88.7(4)*
L($nn) + 1$)–Ru(n)–L($nn - 1$)	*111.2(2)*	*110.6(4)*	*103.1(4)*

Table 11(b)

Ruthenium environments (**4k-Ru**). r is the ruthenium–other atom distance (Å); other entries in the matrices are the angles subtended at the ruthenium by the relevant atoms at the head of the row and column.

Ru(1)

Atom	r	Ru(3)	C(AU)	C(AD)	P(A)	P(B)
Ru(2)	2.857(2)	60.05(6)	77.9(4)	95.6(4)	97.8(1)	150.7(2)
Ru(3)	2.877(3)		92.8(4)	73.9(4)	156.3(1)	91.8(2)
C(AU)	1.94(1)			166.7(5)	90.2(4)	97.0(4)
C(AD)	1.89(1)				102.4(5)	82.8(5)
P(A)	2.301(5)					111.2(2)
P(B)	2.565(9)					

Ru(1)...Ru(2′,3′) are 1.869(3), 1.406(3) Å

Ru(2)

Atom	r	Ru(1)	C(AD′)	C(B)	P(B′)	C(E)
Ru(3)	2.869(3)	60.31(6)	62.4(4)	95.0(4)	101.8(3)	142.1(4)
Ru(1)	2.857(2)		90.5(4)	71.6(4)	160.5(3)	89.0(4)
C(AD′)	2.14(1)			156.6(6)	87.1(4)	99.3(6)
C(B)	2.02(2)				104.7(5)	95.4(6)
P(B′)	2.197(6)					110.6(4)
C(E)	1.82(1)					

Ru(2)...Ru(1′,3′) are 1.869(3), 1.724(3) Å

Ru(3)

Atom	r	Ru(2)	C(B′)	C(AU′)	C(E′)	P(A′)
Ru(1)	2.877(3)	59.64(6)	75.3(4)	94.9(4)	93.5(4)	162.5(1)
Ru(2)	2.869(3)		101.4(4)	70.4(4)	147.6(4)	106.0(1)
C(B′)	2.13(2)			169.8(5)	87.2(6)	99.7(4)
C(AU′)	2.01(1)				96.7(6)	88.7(4)
C(E′)	1.99(1)					103.1(4)
P(A′)	2.292(5)					

Ru(3)...Ru(1′,2′) are 1.406(3), 1.724(3) Å

Ru(3)...C(1D′) is 2.67(2) Å

For carbonyls AU; AD; B; E, respectively: r(C–O) is 1.11(2); 1.14(2); 1.11(2); 1.10(2) Å Ru–C–O is 163(1), 155(1) (Ru(1,3′); 154(1), 150(1), (Ru(1,2′); 154(1), 155(1) (Ru(2,3′)); 155(1), 152(1)° (Ru(2,3′)) Deviations δ(C) from the Ru$_3$ plane are −1.86; 1.74; 1.83; −0.72 Å δP(A,B) are 0.352, −0.378 Å

Table 12

Ruthenium environments (**4m-Ru**)

	$n = 1$	$n = 2$	$n = 3$
Distances (Å)			
$Ru(n)-Ru(n+1)$	2.865(2)	2.848(2)	2.857(1)
$Ru(n)-C(nU)$	1.89(1)	1.97(1)	1.94(1)
$Ru(n)-C(nD)$	1.90(1)	1.93(1)	1.92(1)
$Ru(n)-L(nn+1)$	*2.269(4)*	*2.254(4)*	1.88(1)
$Ru(n)-L(nn-1)$	*2.272(3)*	1.87(1)	*2.261(4)*
Angles (degrees)			
$Ru(n)-1)-Ru(n)-Ru(n+1)$	59.70(3)	60.01(4)	60.29(4)
$Ru(n-1)-Ru(n)-C(nU)$	92.8(4)	94.1(2)	100.9(4)
$Ru(n-1)-Ru(n)-C(nD)$	78.8(4)	76.8(4)	68.2(4)
$Ru(n-1)-Ru(n)-L(nn+1)$	*159.5(1)*	*160.3(1)*	146.4(4)
$Ru(n-1)-Ru(n)-L(nn-1)$	*100.0(1)*	99.1(4)	*108.8(1)*
$Ru(n+1)-Ru(n)-C(nU)$	79.3(4)	71.6(4)	81.2(4)
$Ru(n+1)-Ru(n)-C(nD)$	94.7(4)	99.4(4)	93.7(4)
$Ru(n+1)-Ru(n)-L(nn+1)$	*102.3(1)*	*104.8(1)*	93.7(4)
$Ru(n+1)-Ru(n)-L(nn-1)$	*157.0(1)*	150.6(4)	*163.8(1)*
$C(nU)-Ru(n)-C(nD)$	171.5(5)	169.7(5)	169.0(6)
$C(nU)-Ru(n)-L(nn+1)$	*93.1(4)*	*92.2(4)*	95.0(6)
$C(nU)-Ru(n)-L(nn-1)$	*92.0(4)*	91.1(6)	*89.8(4)*
$C(nD)-Ru(n)-L(nn+1)$	*94.1(4)*	*95.0(6)*	95.1(6)
$C(nD)-Ru(n)-L(nn-1)$	*91.3(4)*	95.0(4)	*92.6(4)*
$L(nn+1)-Ru(n)-L(nn-1)$	*99.4(1)*	99.4(4)	*100.5(4)*
Disordered core			
Distances (Å)			
$Ru(n)-Ru(nn+1)$	1.683(7)	1.575(7)	1.668(7)
$Ru(n)-Ru(nn-1)$	1.604(7)	1.659(7)	1.691(6)
$Ru(nn+1)-Ru(n+1, n+2)$	2.83(1)	2.86(1)	2.85(1)
Angles (degrees)			
$Ru(n-1, n)-Ru(nn+1)-$			
$Ru(n+1, n+2)$	60.6(2)	60.1(2)	59.2(2)
Carbonyl distances (Å) ($\delta(C)$ is the deviation from the Ru_3 plane)			
$C(nU)-O(nU)$	1.16(1)	1.12(2)	1.10(1)
$C(nD)-O(nD)$	1.13(1)	1.16(2)	1.14(1)
$C(nn+1)-O(nn+1)$	–	–	1.13(2)
$C(nn-1)-O(nn-1)$	–	1.11(2)	–
$\delta(C(nU))$	– 1.830	– 1.800	– 1.823
$\delta(C(nD))$	1.824	1.777	1.696
$\delta(C, P(nn+1))$	*0.408*	*0.511*	0.717
$\delta(C, P(nn-1))$	– 0.448	– 0.699	– 0.488
Carbonyl angles (degrees)			
$Ru(n)-C(nU)-O(nU)$	171 (1)	171 (1)	166 (1)
$Ru(n)-C(nD)-O(nD)$	175 (1)	164 (1)	171 (1)
$Ru(n)-C(nn+1)-O(nn+1)$	–	–	172 (1)
$Ru(n)-C(nn-1)-O(nn-1)$	–	175 (1)	–

Deviations of Ru(12,23,31) from the Ru_3 plane are
-0.006, -0.021, -0.017 Å

Acknowledgements

References

1 M.I. Bruce, M.J. Liddell, C.A. Hughes, B.W. Skelton and A.H. White, J. Organomet. Chem., 347 (1988) 157.
2 M.I. Bruce, M.J. Liddell, C.A. Hughes, J.M. Patrick, B.W. Skelton and A.H. White, J. Organomet. Chem., 347 (1988) 181.
3 C.A. Hughes, B.W. Skelton, A.H. White, M.I. Bruce, M.J. Liddell and O. bin Shawkataly, J. Organomet. Chem., 347 (1988) 207.
4 F. Klanberg and E.L. Muetterties, J. Am. Chem. Soc., 90 (1968) 3296.
5 C.A. Udovich and R.J. Clark, J. Organomet. Chem., 36 (1972) 355.
6 M.I. Bruce, G. Shaw and F.G.A. Stone, J. Chem. Soc. Dalton Trans., (1972) 2094.
7 M.I. Bruce, J.G. Matisons and B.K. Nicholson, J. Organomet. Chem., 247 (1983) 321.
8 M.I. Bruce, J.G. Matisons, J.M. Patrick, A.H. White and A.C. Willis, J. Chem. Soc., Dalton Trans., (1985) 1223.
9 G. Lavigne and J.-J. Bonnet, Inorg. Chem., 20 (1981) 2713; G. Lavigne, N. Lugan and J.-J. Bonnet, Organometallics, 1 (1982) 1040.
10 B. Amburani, S. Chawla and A. Poë, Inorg. Chem., 24 (1985) 2635.
11 D.A. Brandes and R.J. Puddephatt, Inorg. Chim. Acta, 113 (1986) 17.
12 J.A. Clucas, D.F. Foster, M.M. Harding and A.K. Smith, J. Chem. Soc., Dalton Trans., (1987) 277.
13 M.I. Bruce, T.W. Hambley, B.K. Nicholson and M.R. Snow, J. Organomet. Chem., 235 (1982) 83.
14 J.A. Clucas, R.H. Dawson, P.A. Dolby, M.M. Harding, K. Pearson and A.K. Smith, J. Organomet. Chem., 311 (1986) 153.
15 W.R. Cullen and D.A. Harbourne, Inorg. Chem., 9 (1970) 1839.
16 S. Cartwright, J.A. Clucas, R.H. Dawson, D.F. Foster, M.M. Harding and A.K. Smith, J. Organomet. Chem., 302 (1986) 403.
17 J.P. Candlin and A.C. Shortland, J. Organomet. Chem., 16 (1986) 289.
18 R.F. Alex and R.K. Pomeroy, J. Organomet. Chem., 284 (1985) 379; Organometallics, 6 (1987) 2437.
19 R.F. Alex, F.W.B. Einstein, R.H. Jones and R.K. Pomeroy, Inorg. Chem., 26 (1987) 3175.
20 A.J. Poë and M.V. Twigg, Inorg. Chem., 13 (1974) 2982.
21 R.E. Cobbedick, F.W.B. Einstein, R.K. Pomeroy and E.R. Spetch, J. Organomet. Chem., 195 (1980) 77.
22 M.R. Churchill, F.J. Hollander and J.P. Hutchinson, Inorg. Chem., 16 (1977) 2655.
23 J.W. Lauher, J. Am. Chem. Soc., 108 (1986) 1526.
24 F.A. Cotton, Prog. Inorg. Chem., 21 (1976) 1.
25 R.H. Crabtree and M. Lavin, Inorg. Chem., 25 (1986) 805.
26 B.E. Mann, in G. Wilkinson, F.G.A. Stone and E.W. Abel (Ed.), Comprehensive Organometallic Chemistry, Pergamon, Oxford, 1982, Vol. 3, p. 151.
27 B.E. Hanson and E.C. Lisic, Inorg. Chem., 25 (1986) 716.
28 D. Braga and B.T. Heaton, J. Chem. Soc., Chem. Commun., (1987) 608.
29 I. Brüdgam, H. Hartl and D. Lentz, Z. Naturforsch. B, 39 (1984) 721.
30 M.R. Churchill and H.R. Wasserman, Inorg. Chem., 21 (1982) 825.
31 A. Bino, F.A. Cotton, P. Lahuerta, P. Puebla and R. Uson, Inorg. Chem., 19 (1980) 2357.
32 T. Venäläinen and T. Pakkanen, J. Organomet. Chem., 266 (1984) 269.
33 T. Chin-Choy, N.L. Keder, G.D. Stucky and P.C. Ford, J. Organomet. Chem., 346 (1988) 225.
34 M.I. Bruce, J.G. Matisons, B.W. Skelton and A.H. White, J. Chem. Soc., Dalton Trans., (1983) 2375.
35 F.A. Cotton, B.E. Hanson and J.D. Jamerson, J. Am. Chem. Soc., 99 (1977) 6588.
36 J.J. de Boer, J.A. van Doorn and C. Masters, J. Chem. Soc. Chem. Commun., (1978) 1005.
37 C.E. Anson, R.E. Benfield, A.W. Bott, B.F.G. Johnson, D. Braga and E.A. Marseglia, J. Chem. Soc., Chem. Commun., (1988) 889.

38 Os$_3$(CO)$_{11}$(CNBu^t): M.I. Bruce, G.N. Pain, C.A. Hughes, J.M. Patrick, B.W. Skelton and A.H. White, J. Organomet. Chem., 307 (1986) 343.

39 Fe$_3$(μ-CO)$_2$(CO)$_9$(NCC$_6$H$_4$Me-2): C.J. Cardin, D.J. Cardin, N.B. Kelly, G.A. Lawless and M.B. Power, J. Organomet. Chem., 341 (1988) 447; Os$_3$(CO)$_{12-n}$(NCMe)$_n$ (n = 1, 2): P.A. Dawson, B.F.G. Johsnon, J. Lewis, J. Puga, P.R. Raithby and M.J. Rosales, J. Chem. Soc., Dalton Trans., (1982) 233.

40 Fe$_3$(μ-CO)$_2$(CO)$_9$(CNBu^t): M.I. Bruce, T.W. Hambley and B.K. Nicholson, J. Chem. Soc., Dalton Trans., (1983) 2385; Ru$_3$(CO)$_{11}$(CNBu^t): M.I. Bruce, J.G. Matisons, R.C. Wallis, J.M. Patrick, B.W. Skelton and A.H. White, J. Chem. Soc., Dalton Trans., (1983) 2365.

41 C.A. Tolman, Chem. Rev., 77 (1977) 313.

42 G. Süss-Fink, M.A. Pellinghelli and A. Tiripicchio, J. Organomet. Chem., 320 (1987) 101.